

Research Article

UCH-L1 inhibitor LDN-57444 hampers mouse oocyte maturation by regulating oxidative stress and mitochondrial function and reducing ERK1/2 expression

Pan Yuan¹, Li Zhou², Xiaona Zhang³, Lan Yao², Jun Ning², Xiao Han², Caifeng Ming¹, Yunhe Zhao² and  Liqun Zhang²

¹Center for Prenatal Diagnosis of Reproductive Medicine, The First Hospital of Jilin University, Changchun 130021, China; ²Department of Gynaecology and Obstetrics, The First Hospital of Jilin University, Changchun 130021, China; ³Department of Anesthesiology, The First Hospital of Jilin University, Changchun 130021, China

Correspondence: Liqun Zhang (zliq@jlu.edu.cn)



Oocyte maturation is a prerequisite for successful fertilization and embryo development. Incomplete oocyte maturation can result in infertility. Ubiquitin carboxy-terminal hydrolase L1 (UCH-L1) has been found to be implicated in oocyte maturation and embryo development. However, the cellular and molecular mechanisms of UCH-L1 underlying oocyte maturation have not been fully elucidated. In the present study, we observed that the introduction of UCH-L1 inhibitor LDN-57444 suppressed first polar body extrusion during mouse oocyte maturation. The inhibition of UCH-L1 by LDN-57444 led to the notable increase in reactive oxygen species (ROS) level, conspicuous reduction in glutathione (GSH) content and mitochondrial membrane potential (MMP), and blockade of spindle body formation. As a conclusion, UCH-L1 inhibitor LDN-57444 suppressed mouse oocyte maturation by improving oxidative stress, attenuating mitochondrial function, curbing spindle body formation and down-regulating extracellular signal-related kinases (ERK1/2) expression, providing a deep insight into the cellular and molecular basis of UCH-L1 during mouse oocyte maturation.

Introduction

Oocytes, female gametocytes or germ cells involved in reproduction, can transmit maternal nuclear and mitochondrial genome information to the embryo and determine embryo developmental potential in women [1]. Oocyte maturation is a physiological event ahead of successful fertilization and embryo development, and failure of or incomplete oocyte maturation can bring about infertility [2]. Most mammalian oocytes are usually arrested at the diplotene stage of prophase I (germinal vesicle (GV) stage) prior to ovulation. During each reproductive cycle, preovulatory luteinizing hormone outpouring induces meiosis resumption and progression till oocyte maturation (metaphase II (MII) stage). After meiosis resumption, oocytes undergo a sequential series of changes, including GV breakdown (GVBD), chromosome condensation, spindle formation and first polar body extrusion [2,3]. *In vitro* maturation (IVM) of immature oocytes, a vital technique in fertility preservation, has attracted much attention from researchers in recent years due to its specific advantages [4,5]. For example, this technique requires no or little gonadotropin supplementation *in vivo*, which can significantly reduce ovarian hyperstimulation syndrome risk, medical expenses and drug-related side effects [5,6]. Despite the great advances in oocyte IVM technique, there are still a lot of controversial issues that need to be addressed [7]. An in-depth understanding on cellular and molecular basis of oocyte IVM contributes to fertility protection, pregnancy rate improvement and the better management of ovarian hyperstimulation syndrome and infertility.

Received: 29 April 2020
Revised: 05 October 2020
Accepted: 06 October 2020

Accepted Manuscript online:
08 October 2020
Version of Record published:
30 October 2020

Mitochondria, cellular organelles responsible for ATP synthesis, play vital roles in various biological processes such as metabolism, calcium homeostasis and cell apoptosis [8]. Mitochondria dysfunction can influence oocyte quality, maturation and fertilization, resulting in the deterioration of reproductive outcomes. Moreover, oocyte mitochondria are the major energy suppliers in the process of preimplantation embryonic development [9]. Furthermore, some studies pointed out that mature oocytes with reduced mitochondrial membrane potential (MMP) had limited sperm penetrability and impaired fertilization competence [10–12]. In addition, mitochondria are the major sites of reactive oxygen species (ROS) production [13] and mitochondrial dysfunction is closely related with the dynamic change of ROS level in oocytes [12]. Additionally, previous studies showed that ROS contributed to oocyte maturation under physiological conditions, while ROS over-production or antioxidant loss could influence oocyte quality and developmental competence, giving rise to anovulation [14]. For instance, a moderate elevation of ROS level contributed to meiotic resumption from diplotene and M-II arrest phases, and excessive ROS generation blocked meiotic cell cycle progression and induced cell apoptosis in oocytes [15,16]. Recently, a growing body of evidence suggests that oocyte mitochondria function improvement and mitochondria replacement might be used for elevating reproductive capability and treating for mitochondrial diseases [9,12].

Ubiquitin carboxy-terminal hydrolase L1 (UCH-L1), also named as pGp 9.5, can function as a deubiquitinating enzyme in monomeric form and an ubiquitin ligase in dimer or oligomeric form [17]. Abnormal expression of UCH-L1 has been reported to be implicated in the pathogenesis of multiple diseases such as cancers [18], nervous system diseases [19] and lung injury [20]. Moreover, previous studies showed that UCH-L1 was selectively and abundantly expressed in multiple reproductive cells such as oocytes, spermatogonia and testis cells [21]. In addition, UCH-L1 has been found to be involved in the regulation of oocyte maturation and embryo development [22,23]. However, the molecular mechanisms of UCH-L1 underlying oocyte maturation have not been fully elucidated.

Methods

Oocyte preparation and IVM

All mouse procedures were performed in Jilin University and approved by Animal Care and Use Committee of Jilin University. The experiments were conducted in accordance with the institutional guidelines of the National Institutes of Health Guide for the Care and Use of Laboratory Animals.

ICR female mice (7-week-old, 20–30 g) were purchased from Laboratory Animal Center of Zhengzhou University (Zhengzhou, China) and fed for ~1 week under a standard condition to allow them to acclimatize. Then, the mice were superovulated by the intraperitoneal injection of 5 IU of pregnant mares' serum gonadotrophin (PMSG; Amyjet Scientific, Beijing, China). After 48 h, mice were killed using intraperitoneal phenobarbital injection (150 mg/kg; Guangdong Bangmin Pharmaceutical Co., Ltd.) and ovaries were removed.

After the removal of excessive tissues and fat under a microscope using the tweezers, oocytes were isolated from ovaries through vigorous poking using a disposable syringe containing an 18G needle. Oocytes (diameter: 80–100 μm , round) with an intact and compact cumulus, GV structure in the center and thick zona pellucida were maintained in drops of M16 medium (Sigma–Aldrich, St. Louis, MO, U.S.A.) covered with mineral oil in a humidified atmosphere containing 5% CO_2 at 37°C. To explore the effect of UCH-L1 inhibition on mouse oocyte maturation, 20 μM of LDN-57444 (Selleck, Houston, Texas, U.S.A.) was added into M16 medium as previously described [21]. Then, first polar body extrusion rate was measured at 18 h after LDN-57444 or DMSO treatment.

ROS level determination

ROS level was measured using the 6-carboxy-2',7'-dichlorodihydrofluorescein diacetate (DCHFDA, Thermo Scientific, Rockford, IL, U.S.A.) following the protocols of manufacturer. Briefly, oocytes were incubated with 10 mM of DCHFDA for 30 min at 37°C. Next, samples were imaged with a fluorescent microscope and the fluorescence intensity was quantified using the ImageJ software.

Glutathione level determination

Glutathione (GSH) level was determined using 10 mM of CellTracker™ Blue CMF2HC Dye (4-chloromethyl-6,8-difluoro-7-hydroxycoumarin) (Thermo Scientific) in oocytes at 18 h after DMSO or LDN-57444 treatment. Samples were imaged with a fluorescent microscope and the fluorescence intensity was quantified using the ImageJ software.

MMP analysis

After three washes with PBS containing 1% polyvinyl alcohol (PBS-PVA), mature oocytes were incubated with 2 mM of tetraethylbenzimidazolylcarbocyanine iodide (JC-1) fluorescent probe (Thermo Scientific) in PBS-PVA solution for 30 min at 37°C. Next, Red and Green fluorescence intensity was rescored using a fluorescent microscope and quantified through ImageJ software after three washes with PBS-PVA. Finally, the ratio of Red/Green fluorescence intensity was calculated to determinate MMP changes with high value of Red/Green fluorescence intensity ratio as the indicator of MMP increase.

Spindle abnormality detection

After washing thrice with PBS-PVA solution, matured oocytes were fixed with 3.7% paraformaldehyde (diluted in PBS-PVA solution) for 30 min and permeabilized for 15 min at 37°C using the 1% Triton X-100 solution. After blocking with PBS-PVA blocking buffer containing 1% BSA for 1 h at room temperature, these oocytes were incubated overnight with FITC-conjugated α -tubulin antibody (Abcam, Cambridge, U.K.) in blocking buffer. Next, these oocytes were stained with 10 μ g/ml of Hoechst 33342 (blue) in PBS to visualize DNA. After three washes with PBS-PVA buffer, samples were mounted on microscope slide and imaged using a Confocal Laser-scanning Microscope (Zeiss LSM 700 META, Jena, Germany). Finally, the intensity of fluorescence signals was analyzed using ImageJ software.

Western blot assay

At 18 h after DMSO or LDN-57444 treatment, total proteins were extracted from oocytes using the RIPA lysis buffer (Beyotime, Shanghai, China) containing protease inhibitors (Thermo Scientific, Waltham, MA, U.S.A.) and quantified using the PierceTM BCA Protein Assay Kit (Thermo Scientific). Next, an equal amount of proteins (30 μ g/lane) were separated through 10% sodium dodecyl sulfate/polyacrylamide gel electrophoresis (SDS/PAGE) and transferred to polyvinylidene fluoride (PVDF) membranes (Millipore, Bedford, MA, U.S.A.). Subsequently, the membranes were blocked for 1 h at room temperature with 5% skim milk and probed overnight at 4°C with primary antibodies against UCH-L1 (#13179, Cell Signaling Technology, Danvers, MA, U.S.A.), extracellular signal-related kinases (ERK1/2; ab17942, Abcam) and glyceraldehyde phosphate dehydrogenase (GAPDH) (ab181602, Abcam). After incubating for 1 h at room temperature with horseradish peroxidase (HRP) conjugated goat anti-rabbit secondary antibody (ab205718, Abcam), the membranes were exposed with PierceTM ECL Western Blotting Substrate (Thermo Fisher Scientific). Finally, the intensity of protein signals was estimated using the Quantity One software Version 4.1.1 (Bio-Rad Laboratories, Hercules, CA, U.S.A.).

Reverse transcription-polymerase chain reaction (RT-qPCR) assay

Total RNA was extracted from oocytes using TRIzol reagent (Thermo Scientific) following the manufacturer's instructions. RNA was reversely transcribed into cDNA using SuperScript III reverse transcriptase (Thermo Scientific). Quantitative PCR analysis was performed using SYBRTM Green PCR Master Mix (Thermo Scientific) and PCR primers on ABI 7500 Real-Time PCR System (Thermo Scientific). Primer sequences were presented as follows: 5'-CTTCAACCCAAACAAGCGCA-3' (forward) and 5'-CCATGTCGAAGGTGAATGGC-3' (reverse) for ERK1; 5'-CCAACCTCTCGTACATCGGA-3' (forward) and 5'-ATGGTTGGTGCCCGGATG-3' (reverse) for ERK2 and 5'-TGTTACCAACTGGGACGACGACA-3' (forward) and 5'-CTGGGTCATCTTTTCACGGT-3' (reverse) for β -actin. β -actin functioned as the internal control to normalize the expression of ERK1/2.

LDN-57444 proteasome activity detection

Proteasome activity is measured using the Proteasome Activity Assay Kit (Abcam, CA, U.S.A.), which principally measures the intensity of highly fluorescent 7-amido-4-methylcoumarin (AMC) released from AMC-tagged peptide substrate (Succ-LLVY-AMC in DMSO) in the presence of proteolytic activity. Briefly, standard curve was prepared using AMC Standard. At 18 h after LDN-57444 treatment, cells were collected and resuspended in 0.5% NP-40 solution. After high-speed centrifugation, cell supernatant was co-incubated with AMC-tagged peptide substrate in the presence or absence of proteasome inhibitor in the dark. Fluorescence was measured at excitation (Ex) wavelength/emission (Em) wavelength = 350/440 nm at 0 and 0.5 h after incubation.

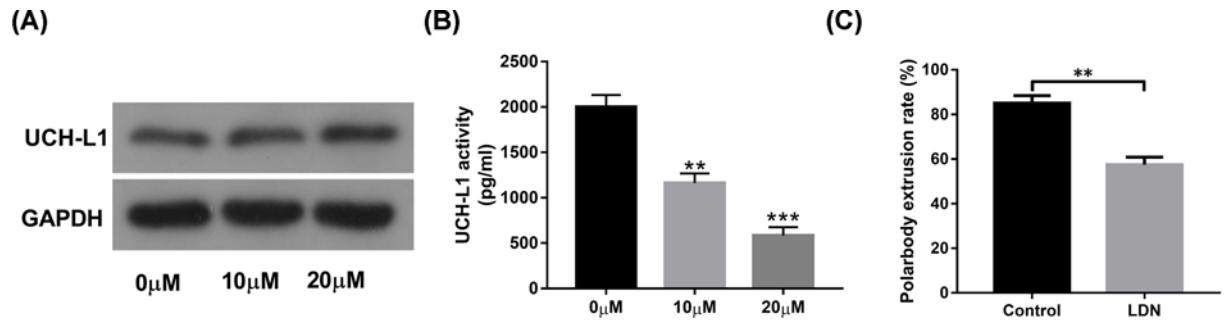


Figure 1. The introduction of UCH-L1 inhibitor LDN-57444 markedly reduced proteasome activity and inhibited mouse oocyte maturation

Mouse oocytes were matured for 18 h in the presence of DMSO (control) or LDN-57444 (10, 20 μM), followed by the measurement of UCH-L1 protein level (A), proteasome activity (B), first polar body extrusion rate (C). ** $P < 0.01$. *** $P < 0.001$.

Statistical analysis

All experiments were repeated at least three times and results were presented as means \pm SEMs. Difference analysis between groups was conducted using unpaired t test with $P < 0.05$ as statistically significant. Difference analysis among groups was performed using one-way ANOVA and Tukey's test.

Results

The introduction of UCH-L1 inhibitor LDN-57444 markedly suppressed mouse oocyte maturation

First, our data revealed that the introduction of LDN-57444 had not much influence on UCH-L1 expression in oocytes (Figure 1A). Since UCH-L1 is a component of ubiquitin proteasome system, the effect of LDN-57444 on proteasome activity was further measured in mouse oocytes. Our outcomes showed that the addition of LDN-57444 led to the notable reduction in proteasome activity (Figure 1B). To explore the cellular and molecular basis of UCH-L1 underlying oocyte maturation, 20 μM of UCH-L1 inhibitor LDN-57444 was used in oocytes as previously described [21,23,24]. Our data revealed that first polar body extrusion rate was notably reduced in LDN-57444-treated oocytes (extrusion rate: 57.47%, $n=98$) than that in control group (extrusion rate: 85.01%, $n=97$) (Figure 1C), suggesting that the inhibition of UCH-L1 proteasome activity by LDN-57444 hindered mouse oocyte maturation.

The introduction of UCH-L1 inhibitor LDN-57444 induced ROS excessive accumulation and caused cellular GSH level reduction in MII phase oocytes

Next, the effect of LDN-57444 on oxidative stress was examined through measuring ROS and GSH levels in MII phase oocytes. H2DCFDA (2',7'-dichlorodihydrofluorescein diacetate) was a cell-permeable probe used to detect intracellular ROS. After diffusing into cells, H2DCFDA is deacetylated by cellular esterases to a non-fluorescent compound, which is later oxidized by ROS into 2',7'-dichlorofluorescein (DCF). DCF is highly fluorescent and is detected by fluorescence spectroscopy with excitation/emission at 495/525 nm. The intensity of green fluorescence was in proportion to ROS level. Our data revealed that ROS level was remarkably increased in LDN-57444 treatment group ($n=111$) relative to control group ($n=110$) (Figure 2A). CellTracker Blue CMF2HC is a fluorescent dye that can freely pass through cell membranes into cells, where it is transformed into cell-impermeant reaction products. In eukaryotic cells, GSH is the most abundant thiol. CMF2HC contains a chloromethyl group that can react with thiol groups, utilizing a glutathione S-transferase-mediated reaction. Hence, the fluorescent intensity of CMF2HC can reflect GSH cellular level. As presented in Figure 2B, GSH level was notably reduced in LDN-57444-stimulated oocytes ($n=75$) versus control group ($n=74$). These outcomes suggested that the inhibition of UCH-L1 by LDN-57444 increased oxidative stress during mouse oocyte maturation.

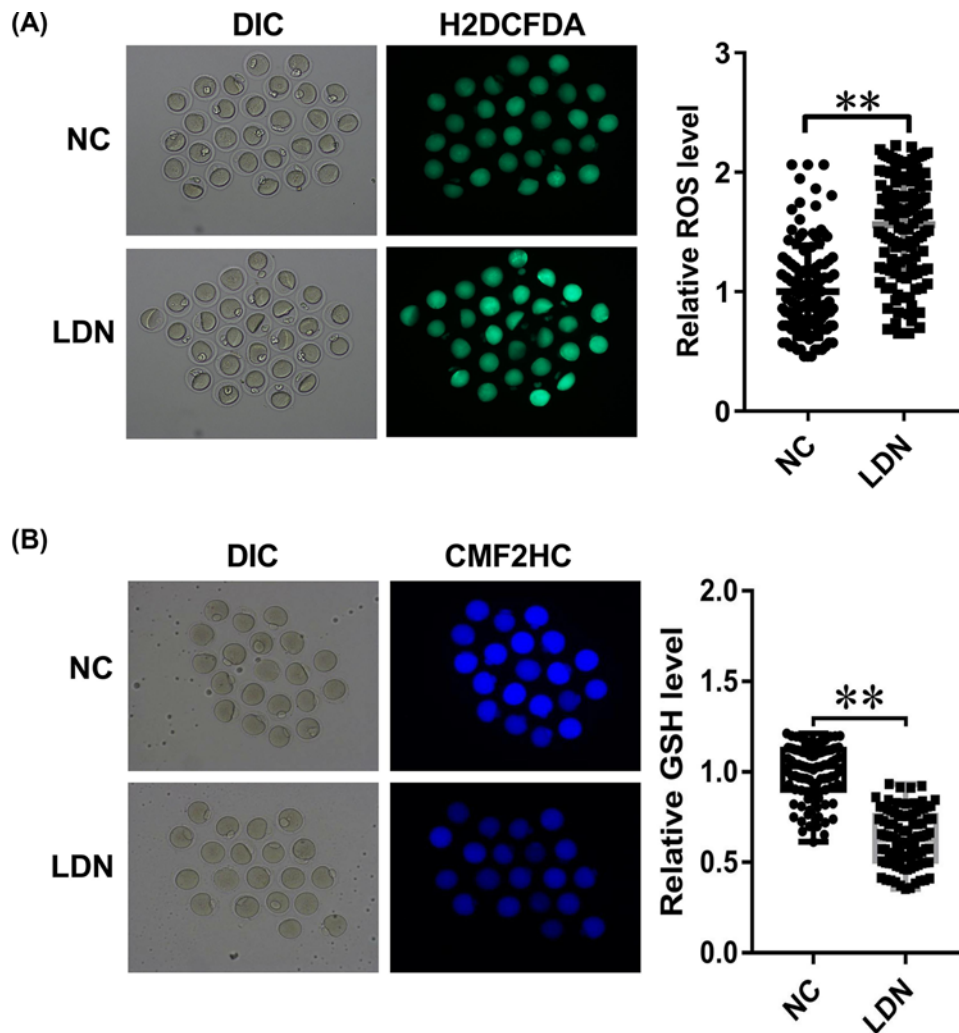


Figure 2. The introduction of UCH-L1 inhibitor LDN-57444 increased oxidative stress during mouse oocyte maturation (A,B) Mouse oocytes were matured with DMSO or LDN-57444 (20 μ M). Eighteen hours later, ROS (A) and GSH (B) levels were determined through corresponding fluorescence probes. $**P < 0.01$.

The introduction of UCH-L1 inhibitor LDN-57444 impaired cellular mitochondria function in MII phase oocytes

MMP has been identified as the crucial indicator of mitochondrial function and cell health. The loss of MMP is a hallmark for apoptosis. It is an early event preceding phosphatidylserine externalization and coinciding with caspase activation.

JC-1 is a cell membrane permeable fluorescent lipophilic carbocyanine dye used to measure MMP. In normal non-apoptotic cells, JC-1 accumulates as aggregates in the mitochondrial in response to high MMP, yielding a red to orange fluorescence. The brightness of red fluorescence is proportional to MMP and varies among different cell types. However, in apoptotic and necrotic cells, which have diminished MMP, JC-1 predominantly exists in the monomer form that yields green fluorescence. Hence, JC-1 Red/Green fluorescence ratio can reflect the level of MMP.

Our study demonstrated that the introduction of UCH-L1 inhibitor LDN-57444 led to the conspicuous reduction in MMP in MII phase oocytes (Figure 3), as evidenced by the reduction in JC-1 Red/Green fluorescence ratio in LDN-57444 treatment group ($n=69$) versus control group ($n=79$), hinting the detrimental effect of UCH-L1 loss on mitochondria function during oocyte maturation.

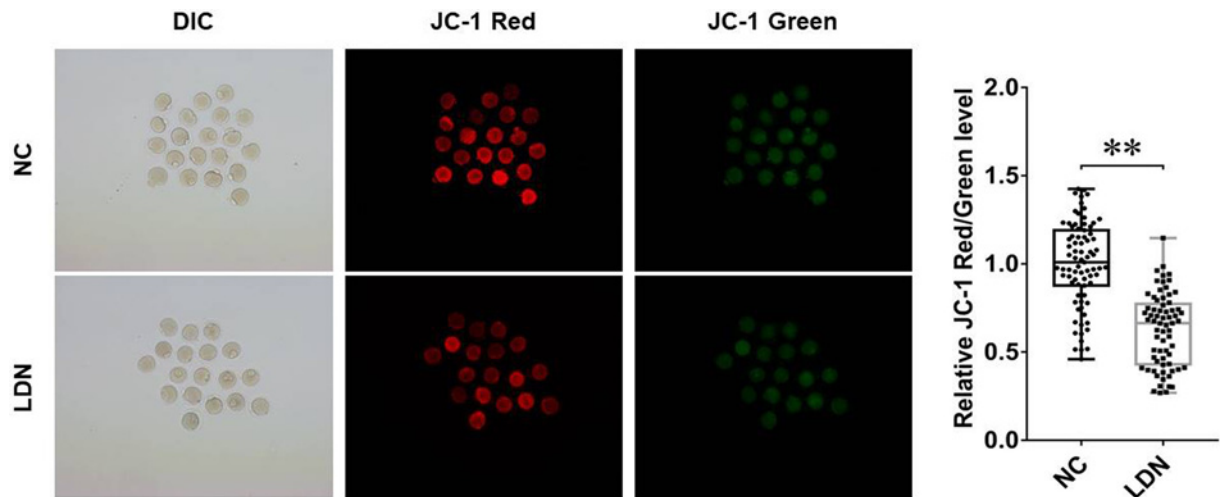


Figure 3. The introduction of UCH-L1 inhibitor LDN-57444 impaired cellular mitochondria function in MII phase oocytes
Mouse oocytes were matured with DMSO or LDN-57444 (20 μ M) for 18 h, followed by the measurement of JC-1 (Red/Green) fluorescence intensity. ** P <0.01.

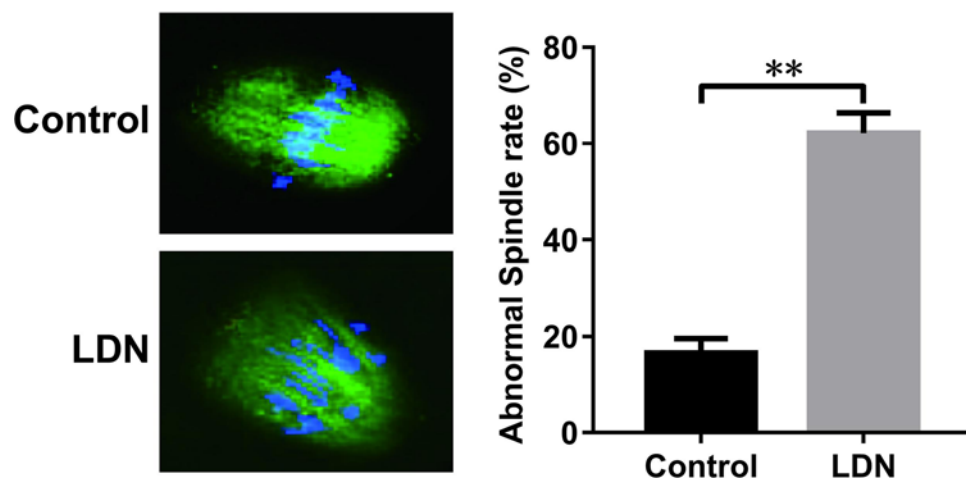


Figure 4. The introduction of UCH-L1 inhibitor LDN-57444 blocked spindle body formation during mouse oocyte maturation
Mouse oocytes were matured with DMSO or LDN-57444 (20 μ M). After 18 h, oocytes were fixed, incubated with FITC-conjugated α -tubulin antibody, stained with Hoechst 33342 solution and analyzed by confocal microscopy. Green, α -tubulin; blue, Hoechst 33342 for DNA staining. ** P <0.01.

The introduction of UCH-L1 inhibitor LDN-57444 blocked spindle body formation during mouse oocyte maturation

α -tubulin, an indispensable constituent of microtubule and spindle body, has been well known as a crucial player in the formation of spindle body. Hence, FITC-conjugated α -tubulin antibody was used to examine whether there were some alteration to spindle body structure in the presence or absence of LDN-57444. As displayed in Figure 4, a higher percentage of microtubule and chromosome misarrangement was observed in LDN-57444-treated oocytes (62.18%, $n=40$) compared with control group (16.56%, $n=42$), suggesting that the introduction of LDN-57444 blocked spindle body formation during mouse oocyte maturation.

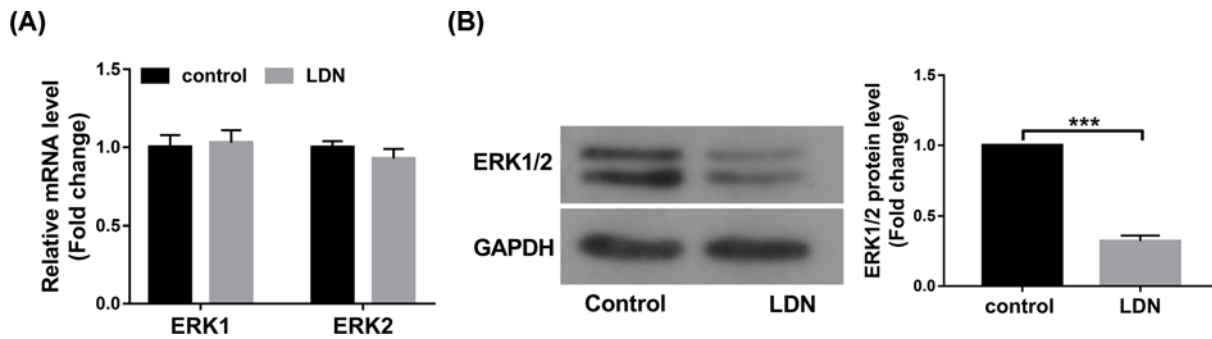


Figure 5. The introduction of UCH-L1 inhibitor LDN-57444 reduced the expression of ERK1/2 protein levels in MII phase oocytes

(A,B) Mouse oocytes were matured with DMSO or LDN-57444 (20 μ M) for 18 h. Then, ERK1/2 mRNA (A) and protein (B) levels were measured through RT-qPCR and Western blot assays, respectively. *** $P < 0.001$.

The introduction of UCH-L1 inhibitor LDN-57444 reduced the expression of ERK1/2 protein levels in MII phase oocytes

Next, we demonstrated that the introduction of LDN-57444 had not much influence on ERK1 and ERK2 mRNA levels in MII phase oocytes (Figure 5A). However, a notable reduction in ERK1/2 protein levels was observed in MII phase oocytes after the stimulation of UCH-L1 inhibitor LDN-57444 (Figure 5B).

Discussion

In the present study, we demonstrated that the introduction of UCH-L1 inhibitor LDN-57444 suppressed mouse oocyte maturation by improving oxidative stress, inducing mitochondrial dysfunction, curbing spindle body formation, and reducing ERK1/2 protein expression.

First, our data revealed that UCH-L1 inhibitor LDN-57444 did not influence UCH-L1 protein expression, but could remarkably reduce UCH-L1 proteasome activity during mouse oocyte maturation. Moreover, the introduction of LDN-57444 led to the notable reduction in first polar body extrusion rate during mouse oocyte maturation, while polar body extrusion is an indicator of oocyte maturation. In other words, our outcomes showed that LDN-57444 inhibited mouse oocyte maturation. Consistent with our results, Susor et al. demonstrated that the inhibition of UCH-L1 by its inhibitor C30 hindered meiotic progression and curbed GVBD in oocytes cultured in maturation medium [22]. The inhibition of UCH-L1 hindered cortical granule (CG) migration, curbed meiotic spindle formation and reduced fertilization rate in porcine oocytes [23]. However, some studies pointed out that the introduction of UCH-L1 inhibitor C16 or C30 did not hamper meiotic progression of bovine oocytes, but induced the increase in polyspermy rate in bovine zygotes after *in vitro* fertilization [24]. Moreover, UCHL1 has been found to be involved in antipolyspermy defense *in vitro* in mouse [25] and pig [26]. In addition, the introduction of UCH-L1 inhibitor LDN-57444 led to the notable elevation in polyspermy and sperm-egg fusion events in zona pellucida-free eggs from superovulated CF-1 female mice [27].

ROS, including peroxides, superoxides, hydroxyl radical and singlet oxygen, can be generated during various biochemical reactions within cells and organelles (e.g. mitochondria and peroxisomes) [28,29]. Recently, ROS has been appreciated as a crucial player in multiple diseases (e.g. male infertility, cancers and neurodegenerative diseases) due to its regulatory effects on cell signaling proteins (e.g. NF- κ B, mitogen-activated protein kinases (MAPKs) and PI3K-Akt), protein kinases and ubiquitination/proteasome system [30–33]. Moreover, ROS and antioxidants play vital roles in the development and maturation of oocytes [14,34]. Antioxidants, including superoxide dismutase (SOD), GSH, catalase and multiple peroxidases, can inhibit ROS over-production and protect oocytes from ROS-mediated detrimental effects in the reproductive system [14]. For instance, previous studies showed that ROS level and DNA damage degree were markedly increased in mouse oocytes exposed to follicular fluid from patients with endometriosis, and the increase in ROS level curbed oocyte maturation in endometriosis [35]. GSH mitigated cadmium-triggered porcine oocyte meiotic defects (e.g. the abnormality of spindle organization, chromosome alignment and actin polymerization, and disruption of mitochondrial integrity and cortical granules dynamics) through reducing ROS level, lessening DNA damage and inhibiting cell apoptosis [36]. Also, a prior document demonstrated that UCH-L1 over-expression facilitated cell invasion through increasing cellular ROS and H₂O₂ levels via deubiquitinating NADPH

oxidase 4 (NOX4) in murine metastatic melanoma (B16F10) cells [37], suggesting the correlation of UCH-L1 and oxidative stress. Our data showed that the inhibition of UCH-L1 by LDN-57444 led to the substantial accumulation of ROS and remarkable reduction in GSH level in MII phase oocytes.

Next, we demonstrated that MMP was markedly reduced in MII phase oocytes following the introduction of UCH-L1 inhibitor LDN-5744, suggesting that the inhibition of UCH-L1 impaired mitochondrial function. Lee et al. demonstrated that the reduction in MMP by FCCP (carbonyl cyanide *p*-(tri-fluoromethoxy) phenyl-hydrazone) curbed ATP generation and first polar body extrusion and blocked blastocyst formation with no effect on total cell number and apoptosis during porcine oocyte maturation [38]. Also, Ge et al. demonstrated that FCCP inhibited nuclear maturation, reduced the proportion of oocytes with normal spindle formation and chromosome alignment and evenly distributed mitochondria, and hampered blastocyst formation during mouse oocyte maturation [39].

In addition, our data showed that the inhibition of UCH-L1 led to the abnormal arrangement of α -tubulin and chromosome and hampered spindle body formation during mouse oocyte maturation. Consistently, Bheda et al. showed that UCH-L1 suppressed tubulin polymerization and microtubule formation in transformed cells during mitosis [40]. Kabuta et al. revealed that UCH-L1 could interact with tubulin, and UCH-L1 I93M mutant and carbonyl-modified UCH-L1 facilitated tubulin polymerization [41].

ERK1/2, members of MAPK superfamily, have been found to be closely associated with oocyte maturation [42,43]. For example, a previous study pointed out that ERK1/2 expression was notably reduced in matured bovine oocytes compared with unmaturing or control oocytes [44]. ERK1/2 knockdown led to the disorganization of chromosome separation and abnormal extrusion of polar body 2 during mouse oocyte maturation [45]. In this text, we demonstrated that ERK1/2 protein levels were markedly down-regulated in MII phase oocytes following the introduction of UCH-L1 inhibitor LDN-57444.

Taken together, these data disclosed that the inhibition of UCH-L1 by LDN-57444 hampered mouse oocyte maturation by reducing ROS level and MMP, increasing GSH level, inhibiting spindle formation and reducing ERK1/2 protein level, deepening our understanding on cellular and molecular mechanisms of UCH-L1 underlying mouse oocyte maturation. Our data also suggested the potential values of UCH-L1 loss in reducing oocyte developmental competence, inducing female infertility and hampering embryo development. However, our experimental design was rough and our conclusion needs to be further validated by other experiments. Also, downstream signaling pathways and regulatory molecules require to be further explored.

Data Availability

The data and material presented in this manuscript are available from the corresponding author on reasonable request.

Competing Interests

The authors declare that there are no competing interests associated with the manuscript.

Funding

We appreciate very much the financial support of the Natural Science Foundation of Science and Technology Department of Jilin Province [grant number 20200201476JC].

Author Contribution

Pan Yuan performed the experiments and wrote the manuscript. Li Zhou, Xiaona Zhang, Lan Yao and Jun Ning contributed to the experimental work. Xiao Han, Caifeng Ming and Yunhe Zhao participated in the experimental design and data analysis. Liqun Zhang contributed to the experiments and manuscript revision.

Abbreviations

CMF2HC, 4-chloromethyl-6,8-difluoro-7-hydroxycoumarin; DCF, 2',7'-dichlorofluorescein; DCFHDA/H2DCFDA, 2',7'-dichlorodihydrofluorescein diacetate; ERK1/2, extracellular signal-related kinase; FCCP, carbonyl cyanide *p*-(tri-fluoromethoxy) phenyl-hydrazone; GAPDH, glyceraldehyde phosphate dehydrogenase; GSH, glutathione; GV, germinal vesicle; GVBD, GV breakdown; HRP, horseradish peroxidase; IVM, *in vitro* maturation; JC-1, tetraethylbenzimidazolylcarbocyanine iodide; MAPK, mitogen-activated protein kinase; MMP, mitochondrial membrane potential; MII, metaphase II; NOX4, NADPH oxidase 4; PVA, polyvinyl alcohol; PVDF, polyvinylidene fluoride; ROS, reactive oxygen species; RT-qPCR, reverse transcription-polymerase chain reaction; SDS/PAGE, sulfate/polyacrylamide gel electrophoresis; SOD, superoxide dismutase; UCH-L1, Ubiquitin carboxy-terminal hydrolase L1.

References

- 1 Keefe, D., Kumar, M. and Kalmbach, K. (2015) Oocyte competency is the key to embryo potential. *Fertil. Steril.* **103**, 317–322, <https://doi.org/10.1016/j.fertnstert.2014.12.115>
- 2 Sen, A. and Caiazza, F. (2013) Oocyte maturation: a story of arrest and release. *Front. Biosci.* **5**, 451–477, <https://doi.org/10.2741/S383>
- 3 Lonergan, P. and Fair, T. (2016) Maturation of oocytes in vitro. *Annu. Rev. Anim. Biosci.* **4**, 255–268, <https://doi.org/10.1146/annurev-animal-022114-110822>
- 4 Shirasawa, H. and Terada, Y. (2017) In vitro maturation of human immature oocytes for fertility preservation and research material. *Reprod. Med. Biol.* **16**, 258–267, <https://doi.org/10.1002/rmb2.12042>
- 5 Khalili, M.A., Shahedi, A., Ashourzadeh, S., Nottola, S.A., Macchiarelli, G. and Palmerini, M.G. (2017) Vitrification of human immature oocytes before and after in vitro maturation: a review. *J. Assist. Reprod. Gen.* **34**, 1413–1426, <https://doi.org/10.1007/s10815-017-1005-4>
- 6 Walls, M.L. and Hart, R.J. (2018) In vitro maturation. *Best Pract. Res. Clin. Obstet. Gynaecol.* **53**, 60–72, <https://doi.org/10.1016/j.bpobgyn.2018.06.004>
- 7 Hatirnaz, S., Ata, B. and Hatirnaz, E.S. (2018) Oocyte in vitro maturation: a systematic review. **15**, 112–125
- 8 Duchon, M.R. (2000) Mitochondria and calcium: from cell signalling to cell death. *J. Physiol.* **529**, 57–68, <https://doi.org/10.1111/j.1469-7793.2000.00057.x>
- 9 Elnur, B. and Emre, S. (2015) Oocyte mitochondrial function and reproduction. *Curr. Opin. Obstet. Gynecol.* **27**, 175–181
- 10 Van, B.J. and Davis, P. (2007) Mitochondrial signaling and fertilization. *Mol. Hum. Reprod.* **13**, 759–770
- 11 Lei, T., Guo, N., Tan, M.-h. and Li, Y.-f. (2014) Effect of mouse oocyte vitrification on mitochondrial membrane potential and distribution. *J. Huazhong Univ. Sci. Med.* **34**, 99–102, <https://doi.org/10.1007/s11596-014-1238-8>
- 12 Roth, Z. (2018) Reduction in oocyte developmental competence by stress is associated with alterations in mitochondrial function. *J. Dairy Sci.* **101**, 3642–3654, <https://doi.org/10.3168/jds.2017-13389>
- 13 Shadel, G.S. and Horvath, T.L. (2015) Mitochondrial ROS signaling in organismal homeostasis. *Cell* **163**, 560–569, <https://doi.org/10.1016/j.cell.2015.10.001>
- 14 Kala, M., Shaikh, M.V. and Nivsarkar, M. (2017) Equilibrium between anti-oxidants and reactive oxygen species: a requisite for oocyte development and maturation. *Reprod. Med. Biol.* **16**, 28–35, <https://doi.org/10.1002/rmb2.12013>
- 15 Tiwari, M. and Chaube, S.K. (2016) Moderate increase of reactive oxygen species triggers meiotic resumption in rat follicular oocytes. *J. Obstet. Gynaecol. Res.* **42**, 536–546, <https://doi.org/10.1111/jog.12938>
- 16 Tiwari, M., Prasad, S., Tripathi, A., Pandey, A.N., Singh, A.K., Shrivastav, T.G. et al. (2016) Involvement of reactive oxygen species in meiotic cell cycle regulation and apoptosis in mammalian oocytes. *Reactive Oxygen Species* **1**, 110–116, <https://doi.org/10.20455/ros.2016.817>
- 17 Liu, Y., Fallon, L., Lashuel, H.A., Liu, Z. and Lansbury, Jr, P.T. (2002) The UCH-L1 gene encodes two opposing enzymatic activities that affect α -synuclein degradation and Parkinson's disease susceptibility. *Cell* **111**, 209–218, [https://doi.org/10.1016/S0092-8674\(02\)01012-7](https://doi.org/10.1016/S0092-8674(02)01012-7)
- 18 Luo, Y., He, J., Yang, C., Orange, M., Ren, X., Blair, N. et al. (2018) UCH-L1 promotes invasion of breast cancer cells through activating Akt signaling pathway. *J. Cell. Biochem.* **119**, 691–700, <https://doi.org/10.1002/jcb.26232>
- 19 Wang, K.K., Yang, Z., Sarkis, G., Torres, I. and Raghavan, V. (2017) Ubiquitin C-terminal hydrolase-L1 (UCH-L1) as a therapeutic and diagnostic target in neurodegeneration, neurotrauma and neuro-injuries. *Expert Opin. Ther. Targets* **21**, 627–638, <https://doi.org/10.1080/14728222.2017.1321635>
- 20 Epshtein, Y., Wang, H. and Jacobson, J.R. (2019) Role of UCHL1 in radiation-induced lung injury mediated by sphingolipids. *Am. Thorac. Soc.*, <https://doi.org/10.1164/ajrccm-conference.2019.199.1.MeetingAbstracts>
- 21 Šušor, A. (2008) Protein synthesis and protein degradation in mammalian oocyte development. *Univerzita Karlova*. Ph.D. Thesis
- 22 Susor, A., Ellederova, Z., Jelinkova, L., Halada, P., Kavan, D., Kubelka, M. et al. (2007) Proteomic analysis of porcine oocytes during in vitro maturation reveals essential role for the ubiquitin C-terminal hydrolase-L1. *Reproduction* **134**, 559–568, <https://doi.org/10.1530/REP-07-0079>
- 23 Yi, Y.-J., Sutovsky, M., Song, W.-H. and Sutovsky, P. (2015) Protein deubiquitination during oocyte maturation influences sperm function during fertilisation, antipolyspermy defense and embryo development. *Reprod. Fertil. Dev.* **27**, 1154–1167, <https://doi.org/10.1071/RD14012>
- 24 Susor, A., Liskova, L., Toralova, T., Pavlok, A., Pivonkova, K., Karabinova, P. et al. (2010) Role of ubiquitin C-terminal hydrolase-L1 in antipolyspermy defense of mammalian oocytes. *Biol. Reprod.* **82**, 1151–1161, <https://doi.org/10.1095/biolreprod.109.081547>
- 25 Sekiguchi, S., Kwon, J., Yoshida, E., Hamasaki, H., Ichinose, S., Hideshima, M. et al. (2006) Localization of ubiquitin C-terminal hydrolase L1 in mouse ova and its function in the plasma membrane to block polyspermy. *Am. J. Pathol.* **169**, 1722–1729, <https://doi.org/10.2353/ajpath.2006.060301>
- 26 Yi, Y.-J., Manandhar, G., Sutovsky, M., Li, R., Jonáková, V., Oko, R. et al. (2007) Ubiquitin C-terminal hydrolase-activity is involved in sperm acrosomal function and anti-polyspermy defense during porcine fertilization. *Biol. Reprod.* **77**, 780–793, <https://doi.org/10.1095/biolreprod.107.061275>
- 27 Christianson, M.S., Gerolstein, A.L., Lee, H.J., Monseur, B.C., Robinson, D.N. and Evans, J.P. (2016) Effects of Ubiquitin C-terminal hydrolase L1 (UCH-L1) inhibition on sperm incorporation and cortical tension in mouse eggs. *Mol. Reprod. Dev.* **83**, 188–189, <https://doi.org/10.1002/mrd.22617>
- 28 Ray, P.D., Huang, B.-W. and Tsuji, Y. (2012) Reactive oxygen species (ROS) homeostasis and redox regulation in cellular signaling. *Cell. Signal.* **24**, 981–990, <https://doi.org/10.1016/j.cellsig.2012.01.008>
- 29 del Río, L.A. and López-Huertas, E. (2016) ROS generation in peroxisomes and its role in cell signaling. *Plant Cell Physiol.* **57**, 1364–1376
- 30 Wagner, H., Cheng, J.W. and Ko, E.Y. (2018) Role of reactive oxygen species in male infertility: an updated review of literature. *Arab J. Urol.* **16**, 35–43, <https://doi.org/10.1016/j.aju.2017.11.001>
- 31 Moloney, J.N. and Cotter, T.G. (2018) ROS signalling in the biology of cancer. *Semin. Cell Dev. Biol.* **80**, 50–64, <https://doi.org/10.1016/j.semcdb.2017.05.023>
- 32 Nissanka, N. and Moraes, C.T. (2018) Mitochondrial DNA damage and reactive oxygen species in neurodegenerative disease. *FEBS Lett.* **592**, 728–742, <https://doi.org/10.1002/1873-3468.12956>

- 33 Zhang, J., Wang, X., Vikash, V., Ye, Q., Wu, D., Liu, Y. et al. (2016) ROS and ROS-mediated cellular signaling. *Oxid. Med. Cell Longev.* **2016**, 4350965, <https://doi.org/10.1155/2016/4350965>
- 34 Khazaei, M. and Aghaz, F. (2017) Reactive oxygen species generation and use of antioxidants during in vitro maturation of oocytes. *Int. J. Fertil. Steril.* **11**, 63
- 35 Hamdan, M., Jones, K., Cheong, Y. and Lane, S. (2016) Oocyte maturation arrest in endometriosis is caused by elevated levels of reactive oxygen species and enforced via a DNA damage response and the spindle assembly checkpoint pathway. *Soc. Reprod. Fertil. Ann. Conference* **2016**, 3
- 36 Zhou, C., Zhang, X., Chen, Y., Liu, X., Sun, Y. and Xiong, B. (2019) Glutathione alleviates the cadmium exposure-caused porcine oocyte meiotic defects via eliminating the excessive ROS. *Environ. Pollut.* **255**, 113194, <https://doi.org/10.1016/j.envpol.2019.113194>
- 37 Kim, H.J., Magesh, V., Lee, J.-J., Kim, S., Knaus, U.G. and Lee, K.-J. (2015) Ubiquitin C-terminal hydrolase-L1 increases cancer cell invasion by modulating hydrogen peroxide generated via NADPH oxidase 4. *Oncotarget* **6**, 16287, <https://doi.org/10.18632/oncotarget.3843>
- 38 Lee, S.-K., Zhao, M.-H., Kwon, J.-W., Li, Y.-H., Lin, Z.-L., Jin, Y.-X. et al. (2014) The association of mitochondrial potential and copy number with pig oocyte maturation and developmental potential. *J. Reprod. Dev.* **60**, 128–135, <https://doi.org/10.1262/jrd.2013-098>
- 39 Ge, H., Tollner, T.L., Hu, Z., Dai, M., Li, X., Guan, H. et al. (2012) The importance of mitochondrial metabolic activity and mitochondrial DNA replication during oocyte maturation in vitro on oocyte quality and subsequent embryo developmental competence. *Mol. Reprod. Dev.* **79**, 392–401, <https://doi.org/10.1002/mrd.22042>
- 40 Anjali, B., Anuradha, G., Michael, C., Pagano, J.S. and Julia, S. (2010) Ubiquitin editing enzyme UCH L1 and microtubule dynamics: implication in mitosis. *Cell Cycle* **9**, 980–994
- 41 Kabuta, T., Setsuie, R., Mitsui, T., Kinugawa, A., Sakurai, M., Aoki, S. et al. (2008) Aberrant molecular properties shared by familial Parkinson's disease-associated mutant UCH-L1 and carbonyl-modified UCH-L1. *Hum. Mol. Genet.* **17**, 1482–1496, <https://doi.org/10.1093/hmg/ddn037>
- 42 Lopez-Cardona, A., Sanchez-Calabuig, M., Beltran-Brena, P., Agirregoitia, N., Rizos, D., Agirregoitia, E. et al. (2016) Exocannabinoids effect on in vitro bovine oocyte maturation via activation of AKT and ERK1/2. *Reproduction* **152**, 603–612, <https://doi.org/10.1530/REP-16-0199>
- 43 Chouzouris, T.-M., Dovolou, E., Krania, F., Pappas, I.S., Dafopoulos, K., Messinis, I.E. et al. (2017) Effects of ghrelin on activation of Akt1 and ERK1/2 pathways during in vitro maturation of bovine oocytes. *Zygote* **25**, 183–189, <https://doi.org/10.1017/S096719941700003X>
- 44 Popelkova, M., Sirotkin, A.V., Bezakova, A., Makarevic, A., Pivko, J., Kacmarik, J. et al. (2006) Effect of IGF-I, leptin, ghrelin and MAPK-ERK on the nuclear maturation of bovine oocytes. *Bull. Vet. Inst. Pulawy* **50**, 179
- 45 Zhang, Y.-L., Liu, X.-M., Ji, S.-Y., Sha, Q.-Q., Zhang, J. and Fan, H.-Y. (2015) ERK1/2 activities are dispensable for oocyte growth but are required for meiotic maturation and pronuclear formation in mouse. *J. Genet. Genom.* **42**, 477–485, <https://doi.org/10.1016/j.jgg.2015.07.004>